

Electronic Supplementary Information

Thermochemical wastewater valorization via enhanced microbial toxicity tolerance

Lahiru N. Jayakody¹, Christopher W. Johnson¹, Jason M. Whitham², Richard J. Giannone², Brenna A. Black¹, Nicholas S. Cleveland¹, William E. Michener¹, Jessica L. Olstad¹, Derek R. Vardon¹, Robert C. Brown³, Dawn M. Klingeman², Steven D. Brown^{2, 4}, Robert L. Hettich², Adam M. Guss², Gregg T. Beckham^{1, *}

¹National Bioenergy Center, National Renewable Energy Laboratory, Golden CO 80401

²Oak Ridge National Laboratory, 1 Bethel Valley Rd, Oak Ridge, TN 37830

³Bioeconomy Institute and Department of Mechanical Engineering, Iowa State University, Ames, IA 50011, USA

⁴LanzaTech, Inc., Skokie, IL 60077, USA

*Email: gregg.beckham@nrel.gov

Supplemental Materials and Methods

Determination of the combinational inhibitory effect of FPF chemical functional groups

A three-level partial factorial growth experiment was performed using synthetic medium containing combinations of the most abundant compounds present in FPF based on their functional groups, including FPF-aldehyde, FPF-ketone, FPF-acids, and FPF-phenolics. Level 1 contained 0 % (v/v), level 2 contained 0.02 % (v/v), and level 3 contained 0.03 % (v/v); 9-interactions were tested according to Taguchi Orthogonal "L" Array design metrics (**ESI Fig. S2**). 200 μ L of M9 medium-containing 20 mM glucose supplemented with various concentrations of FPF components was added to the wells of a Bioscreen C microplate, *P. putida* KT2440 cells were added to reach an initial cell density of $OD_{600}=0.1$, and the plate was incubated at 30°C with medium shaking. The $OD_{420-580}$ was monitored using a Bioscreen C MBR analyzer (Growth Curves US, Piscataway, NJ) every 30 min to generate growth curves. Growth curves were performed in triplicate and the average growth rate was obtained. The data were further subjected to partial least square regression analysis (PLS) with XLSTAT software to obtain the variable important parameter (VIP) of each component.

Sample preparation for RNA-seq and proteomics analysis

Cultures grown in M9-medium-containing 20 mM glucose at 30 °C and 225 rpm were collected in mid log phase and washed twice with M9 medium containing 20 mM glucose and used to inoculate 60 mL of M9 medium-containing 20 mM glucose supplemented with or without 2 mM glycolaldehyde or 0.05% (v/v) FPF in 250 mL baffled flasks to an $OD_{600}=0.1$ and incubated shaking at 225 rpm, 30 °C. Cells were harvested when cells reached mid-log phase, at $OD_{600}=0.5$. 10 mL and 50 mL of each culture were collected from each flask for RNA isolation and protein extraction, respectively. Cells were centrifuged for 5 min at 4,800 rpm, 30 °C, using high speed acceleration and deceleration. The supernatant was discarded, and the cell pellet-containing vials were subjected to liquid nitrogen for 1 min and stored in -80 °C until RNA-seq and proteomic analysis.

RNA isolation: Cell pellets were resuspended in 1.5 ml of TRIzol (Life Technologies, Carlsbad, CA, USA) and total RNA was isolated following the manufacturer's protocol. The aqueous phase was obtained and mixed at a ratio of 1:1 with > 75% ethanol and purified on an RNeasy column (Qiagen, Valencia, CA), including on column DNase treatment, following the manufacturer's protocol. Isolated RNA was measure and assessed for quality on a 2100 Bioanalyzer (Agilent Technologies, Santa Clara, CA) and a Nanodrop-1000 (Thermo Scientific, Waltham, MA). Total RNA was sent to Joint Genome Institute (<http://jgi.doe.gov/>) for cDNA library generation and sequencing.

Sequencing, expression data quality control, normalization, quantification, and differential expression analysis:

Paired-end reads (2 x 151 bp) were generated on a HiSeq-2500 using rapid V2 chemistry, demultiplexed, trimmed, and filtered with BBduk (<https://sourceforge.net/projects/bbmap/>) to remove reads with greater than a single mismatch, without kmer matching (kmer=25), and ones which are known contaminants and PhiX spike-in reads. Only unique reads were mapped with BBMap (<https://sourceforge.net/projects/bbmap/>) to the *Pseudomonas putida* KT2440 genome (IMG OID 637000222). Sequences that mapped to more than one location in the genome, mapped with 93% identity to human, cat, dog and mouse references, mapped to common microbial contaminant references, or ribosomal RNA were removed. featureCounts was used to generate the raw gene counts.¹ Raw read counts were used to evaluate

the level of correlation between biological samples using Pearson's correlation (ESI Materials and Methods). Differential expression analysis was performed with DESeq2 using raw read counts.² Genes were considered significantly differentially expressed when their adjusted p-values were less than or equal to 0.05 and \log_2 -fold change values were ≥ 2 or ≤ -2 . ANOVA analysis was performed in JMP Genomics 8 (SAS Institute, Cary, NC, USA) using FPKM-normalized read counts (fragments per kilobase of open reading frame per million mapped reads). The obtained RNA seq data are available at NCBI bioproject PRJNA398406, SRA submission SRP116349.

GO enrichment analysis: Protein sequences from the *P. putida* KT2440 genome (IMG OID 637000222) were annotated with gene ontology (GO) names after merging of assignments from NCBI Blastp and InterProScan (with applications BlastProDom, FPrintScan, HMMPIR, HMMPfam, HMMSmart, HMMTigr, ProfileScan, HAMAP, PartterScan, SuperFamily, SignalPHMM, TMHMM, HMMPanther, Gene3D, Phobius, Coils, CDD, SFLD, and MobiDBLite). Fisher's Exact Test was performed with differentially expressed genes (\log_2 -fold ≥ 1 or ≤ -1 and FDR < 0.05) and the GO-annotated genome as a reference. All steps were performed with default parameters in the Blast2GO 4.1.5 (Oracle Corporation, Redwood City, CA).

Proteome isolation from whole cells: Whole-cell lysates were prepared by bead beating in sodium deoxycholate lysis buffer (4% SDC, 100 mM ammonium bicarbonate (ABC), 10 mM dithiothreitol, pH 7.8) using 0.15 mm zirconium oxide beads followed by centrifugation at 21,000 x g. Precleared protein lysates were moved to a new microfuge tube, denatured/reduced at 80°C for 10 min, and adjusted to 30 mM iodoacetamide to alkylate cysteines. After 20 min incubation in the dark at room temperature, sample protein concentrations were measured via BCA (Pierce). Protein samples were then transferred to a 10 kDa MWCO spin filter (Vivaspin 500, Sartorius), rinsed with ABC, and digested *in situ* with sequencing-grade trypsin as previously described.³ Tryptic peptides were then collected by centrifugation (10,000 x g), SDC precipitated with 1% formic acid, and precipitate removed from the peptide solution with water-saturated ethyl acetate. Peptide samples were then concentrated via SpeedVac and measured by BCA.

Two-dimensional LC-MS/MS analysis of peptide mixtures: Peptide samples were analyzed by automated 2D LC-MS/MS analysis using a Vanquish UHPLC with autosampler plumbed directly in-line with a Q Exactive Plus mass spectrometer (Thermo Scientific) outfitted with a triphasic back column (RP-SCX-RP; reversed-phase [5 μ m Kinetex C18] and strong-cation exchange [5 μ m Luna SCX] chromatographic resins; Phenomenex) coupled to an in-house pulled nanospray emitter packed with 30 cm Kinetex C18 resin. For each sample, 6 μ g of peptides were autoloading, desalted, separated and analyzed across three successive salt cuts of ammonium acetate (35, 50, and 500 mM), each followed by 105 min organic gradient. Eluting peptides were measured and sequenced by data-dependent acquisition on the Q Exactive as previously described.³

Database searching and proteome informatics: MS/MS spectra were searched with MyriMatch v.2.2 against the *P. putida* KT2440 proteome concatenated with common protein contaminants and reversed entries to estimate false-discovery rates (FDR).⁴ Peptide spectrum matches (PSM) were required to be fully tryptic with any number of missed cleavages; a static modification of 57.0214 Da on cysteine and a dynamic modification of 15.9949 Da on methionine residues. PSMs were filtered using IDPicker v.3.0 with an experiment-wide FDR controlled at < 1% at the peptide-level.⁵ Peptide intensities were assessed by chromatographic area-under-the-curve (label-free quantification option in IDPicker). To remove cases of extreme sequence redundancy, the *P. putida* proteome was clustered at 90% sequence identity (UCLUST) and peptides intensities summed to their respective protein groups/seeds to estimate overall protein abundance.⁶ Protein abundance distributions were then normalized across samples and missing values imputed to simulate the mass spectrometer's limit of detection.

***mcl*-PHAs quantification and characterization**

10-30 mg of cells were added to a glass vial and derivatized by adding ~1 mL of BF₃/MeOH containing 200 μ L of benzoic acid dissolved in dichloromethane (10 mg/mL) as an internal surrogate to track derivatization. The vials were sealed, shaken, placed in a heating block at 80°C overnight, and allowed to cool to room temperature. The samples were moved into a 10 mL volumetric flask and the vial residual was rinsed twice with DCM before filling the flask to 10 mL total with additional DCM. The 10 mL solution was transferred to a PTFE capped vial and ~3 mL of water was added to form a bi-phase and wash out residual BF₃ to the aqueous layer. The DCM layer (~2 mL) was then transferred into another vial containing a small amount of Na₂SO₄ and Na₂CO₃ to dry and neutralize any remaining BF₃. The dried and neutralized solutions were syringe filtered (0.2 μ m PTFE) into fresh vials for analysis. To track recovery of PHAs during sample derivatization and analysis, triplicate biomass samples of *P. putida* KT2440 were processed in parallel. Recovery yields during sample workup were calculated based on a cell dry weight PHA content of 24% determined by bulk sample solvent extraction. Hydroxyacid methyl esters were identified and the distribution quantified by gas chromatography mass spectroscopy (GC-MS) using an Agilent 6890N GC equipped with a 5973

MSD (Agilent Technologies). Agilent MSD Productivity Chemstation G1701 software version D.00.00 was used to collect and quantitate analytes. 8-Hydroxyoctanoic acid, 10-hydroxydecanoic acid, 12-hydroxydodecanoic acid, and 14-hydroxytetradecanoic acids were obtained from Sigma Aldrich (98+% purity, Sigma Aldrich, St. Louis, MO, USA), methylated as per the method used for the samples, and used to determine the GC-MS instrument response. Samples were injected at a volume of 1 μ L onto a Stabilwax-DA column (30 m \times 0.25-mm id, 0.25- μ m film) in splitless mode, with helium at 1 mL/min constant flow used as the carrier gas. The GC/MS method consisted of a front inlet temperature of 250°C, and an auxiliary transfer line temperature of 260°C. The separation used had a starting temperature of 225°C and this was held for 2 min, then ramped at 15°C/min to a temperature of 250°C and held for 5.7 minutes for a total run time of 27 min. Sample total ion counts were collected on the mass spectrometer at scan range from 30 to 450 m/z . Calibration curves were made by diluting the derivatized standards between a concentration of 5-175 μ g/L. A minimum of six calibration levels was used resulting in an r^2 coefficient of 0.995 or better for each analyte and a check calibration standard (CCS) was analyzed every ten samples to insure the integrity of the initial calibration. An internal standard of 1,2-diphenylbenzene (99.9+% purity, AccuStandard, New Haven, CT) was added to all standards and samples at a concentration of 40 μ g/L to adjust for any detector response shift.

High performance liquid chromatography (HPLC) analysis

Concentrations of acetate, glycolaldehyde, furfural, HMF, and glycolate were measured using high performance liquid chromatography (HPLC) by injecting 6 μ L of 0.2- μ m filter-sterilized culture supernatant onto an Agilent 1100 series system (Agilent USA, Santa Clara, CA) equipped with a Phenomenex Rezex RFQ-Fast Fruit H+ column (Phenomenex, Torrance, CA) and cation H+ guard cartridge (Bio-Rad Laboratories, Hercules, CA) at 85°C. A mobile phase of 0.1 N sulfuric acid was used at a flow rate of 1.0 mL/min. Refractive index and diode array detectors were used for compound detection. Compounds were identified by relating the retention times and spectral profiles with standard HPLC grade pure compounds (Sigma Aldrich, St. Louis, MO, USA) and the concentration of each compound was calculated based on a calibration curves generated using pure compounds.

Total carbon analysis

The total carbon of the samples was determined using a LECO TruSpec CHN module (LECO Corporation, Saint Joseph, MI). The sample (nominal weight of 0.1g, encapsulated in a tin foil capsule with Al₂O₃) was placed in the sample loading head, sealed, and purged of any atmospheric gases. The sample was dropped into a furnace dosed with pure O₂ gas (99.995 %) at 950 °C for combustion. The combustion products passed through the afterburner furnace (850 °C), where they succumbed to further oxidation and particulate removal. The resulting gaseous products were sent through anhydrous to remove moisture, and on to a CO₂ infrared detector to determine carbon content.

Western blot (WB) analysis of GFP protein

For the WB analysis, 25 mL of M9 medium supplemented with 20 mM glucose with or without 3 mM GA or 0.1 % (v/v) FPF in a 125 mL baffled flask was inoculated to an OD₆₀₀=0.1 with GFP-expressing strains using log phase pre-cultures made in 20 mM glucose containing M9 medium. Cultures were incubated shaking at 225 rpm, 30 °C, and cells were harvested after 3 h. Soluble fractions of proteins were extracted by using a B-PER solution (Thermo Fisher Scientific Inc, Waltham, MA, USA) according to manufacturer's instructions. Immuno-detection of GFP was accomplished using the SNAP i.d.® 2.0 Protein Detection System (Millipore Corp, USA). SDS-PAGE gels were transferred via standard wet tank transfer to the PVDF membranes. Membranes were blocked using SuperBlockPBS (Thermo Fisher Scientific Inc., Rockford, IL, USA) for 10 min at room temperature and then washed four times for 2 min each in PBS-T buffer (10 mM Na₃PO₄, 0.15M NaCl, 0.05% (v/v) Tween-20, pH 7.5). GFP Tag Monoclonal Antibody (11E5) IgG antibody (Thermo Fisher Scientific Inc., Rockford, IL, USA) was diluted 1:5,000 in blocking buffer, and the blots were incubated for 10 min at room temperature and washed three times with wash buffer. Goat anti-Mouse IgG, IgM (H+L) Cross-Adsorbed Secondary Antibody, AP (Thermo Fisher Scientific Inc., Rockford, IL, USA) was diluted 1:1000 in blocking buffer, added to the PVDF membranes and incubated 10 min. Membranes were washed three times with wash buffer and the alkaline phosphatase localization was visualized using BCIP/NBT (Life Technologies Corp, Carlsbad, CA, USA). The detected GFP protein bands were quantified by using Image J software.⁷

Supplemental Figures and Tables

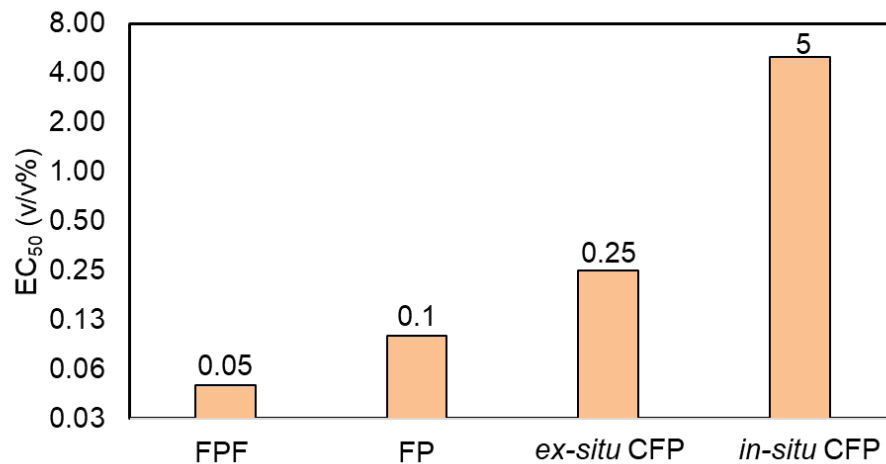


Figure S1. EC₅₀ values of the different TC waste water streams on *P. putida* KT2440. The EC₅₀ value is defined as concentration of TC wastewater (v/v%) in M9 medium containing 20 mM glucose, which is inhibited *P. putida* growth rate by 50%. TC: thermochemical: FP: fast pyrolysis, FPF: fast pyrolysis with fractionation, CFP: catalytic fast pyrolysis.

Table : Fractional factorial experiment design metrics

Run	Concentration (v/v %)				AVG – growth rate (h ⁻¹)	SEM
	FPF _{SYN-Ald}	FPF _{SYN-Ket}	FPF _{SYN-Phe}	FPF _{SYN-Ace}		
1	0.00	0.00	0.00	0.00	0.252	0.002
2	0.00	0.02	0.02	0.02	0.270	0.003
3	0.00	0.03	0.03	0.03	0.257	0.006
4	0.02	0.00	0.02	0.03	0.221	0.004
5	0.02	0.02	0.03	0.00	0.187	0.002
6	0.02	0.03	0.00	0.02	0.187	0.001
7	0.03	0.00	0.03	0.02	0.111	0.001
8	0.03	0.02	0.00	0.03	0.057	0.005
9	0.03	0.03	0.02	0.00	0.230	0.003

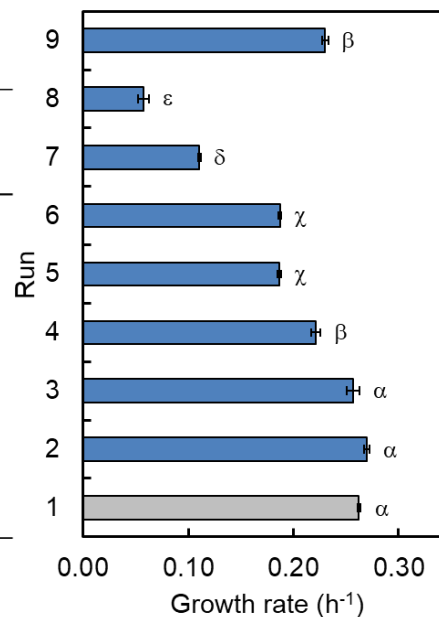


Figure S2. Fractional factorial experiment of combinational inhibitory effects of different functional group compounds found in FPF on *P. putida* KT2440. FPF_{SYN-Ald}: a synthetic medium of aldehydes, FPF_{SYN-Ket}: a synthetic medium of ketones, FPF_{SYN-phe}: a synthetic medium of phenols, and FPF_{SYN-Ace}: a synthetic medium of acids fraction of FPF. Results are expressed as means ± SEM (n=3). Bars labeled with different symbols (α, β, ε, δ, and χ) indicate statistical significance of different run ($p < 0.05$; one-way ANOVA followed by Tukey's post hoc honest significance difference test). Bars labeled with the same symbol(s) indicate no statistically significant difference ($p > 0.05$; one-way ANOVA followed by Tukey's post hoc honest significance difference test). FPF: fast pyrolysis with fractionation, ANOVA: analysis of variance.

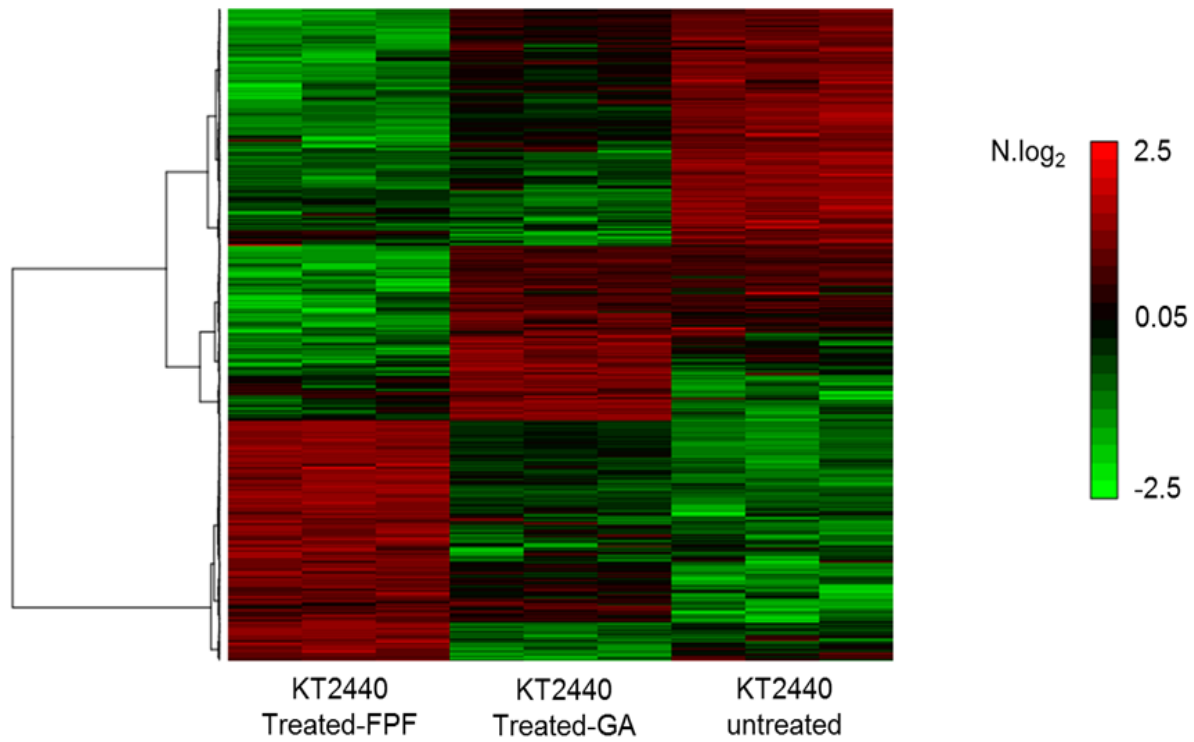


Figure S3. Heat map of the global proteomics profiles of *P. putida* KT2440 untreated or treated with 2 mM GA or 0.05% (v/v) FPF. FPF: fast pyrolysis with fractionation, GA: glycolaldehyde.

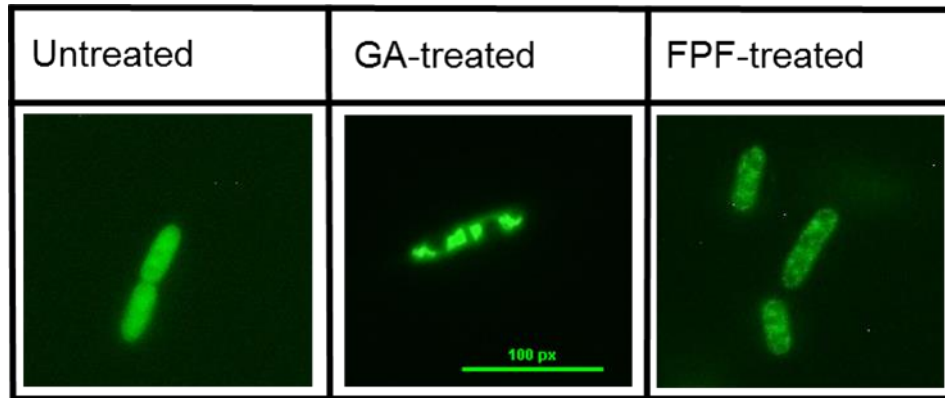


Figure S4. Formation of inclusions body of GFP after treatment of the GFP-expressing *P. putida* KT2440 cells with GA or of FPF. Cells were observed by epifluorescence microscope after 3 h treatment in 20 mM glucose containing M9 medium supplemented with 3 mM GA or 0.05% (v/v) of FPF. FPF: fast pyrolysis with fractionation, GA: glycolaldehyde, GFP: green fluorescent protein.

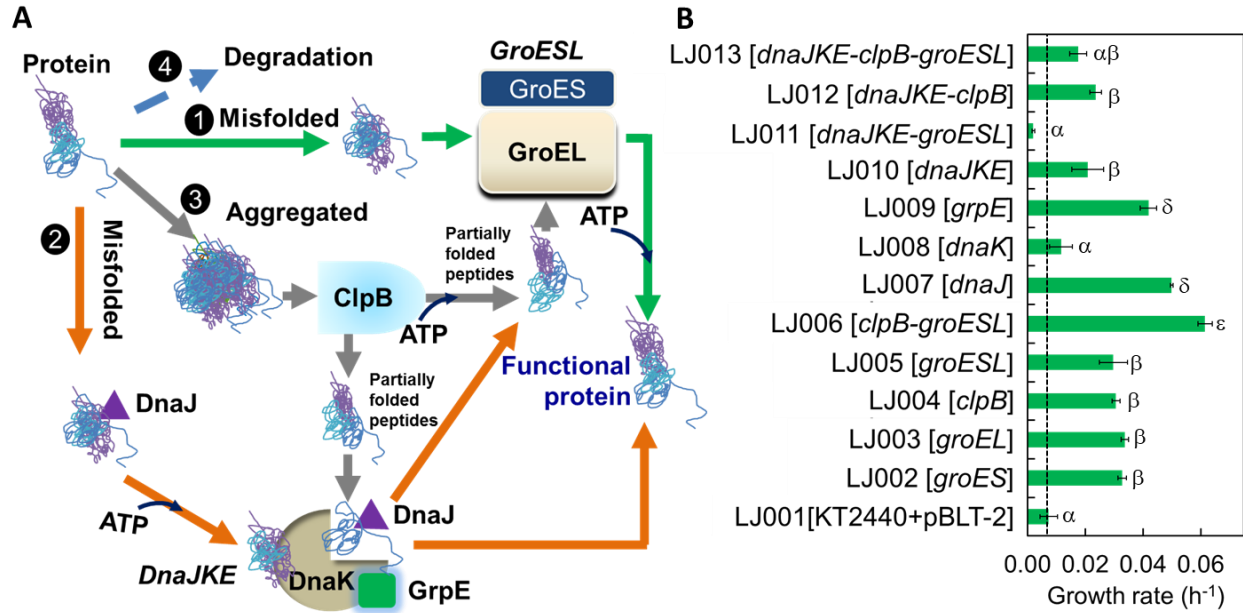


Figure S5. (A) Schematic illustration of the mechanisms of protein recovery by chaperone cascades. Green arrows represent GroES and GroEL dependent (GroESL) misfolded protein recovery, orange arrows represent DnaJ, DnaK, and GrpE dependent (DnaJKE) misfolded protein recovery, and gray arrows represent aggregated protein recovery via ClpB with the assistant of GroESL or/and DnaJKE system. (B) The effect of plasmid-based expression of chaperone protein(s) on tolerance of *P. putida* KT2440 to glycolaldehyde. Bars labeled with different symbols (α , β , and ϵ) indicate statistical significance in the differences in growth rate between those strains ($p < 0.05$; one-way ANOVA followed by Tukey's post hoc honest significance difference test). Bars labeled with the same symbol(s) indicate no statistically significant difference ($p > 0.05$; one-way ANOVA followed by Tukey's post hoc honest significance difference test) FPF: fast pyrolysis with fractionation, ANOVA: analysis of variance. ATP: adenosine triphosphate.



Figure S6. configuration of genomic integrated cassette of synthetic chaperone operon

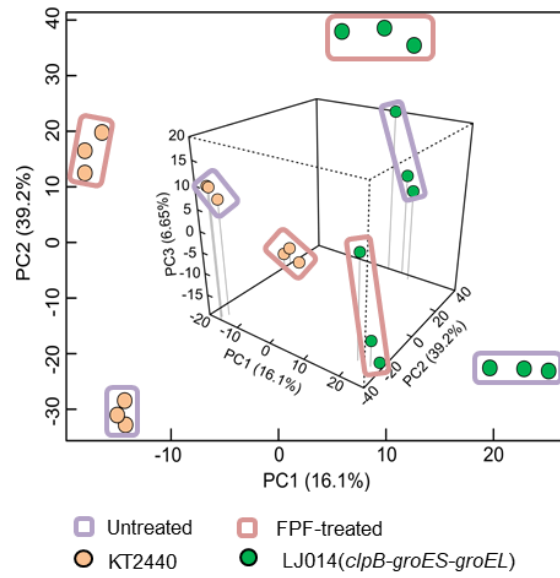


Figure S7. 2D- and 3D-PLS global proteomics plots of the strains with or without treatment of FPF (0.5% v/v). FPF: fast pyrolysis with fractionation.

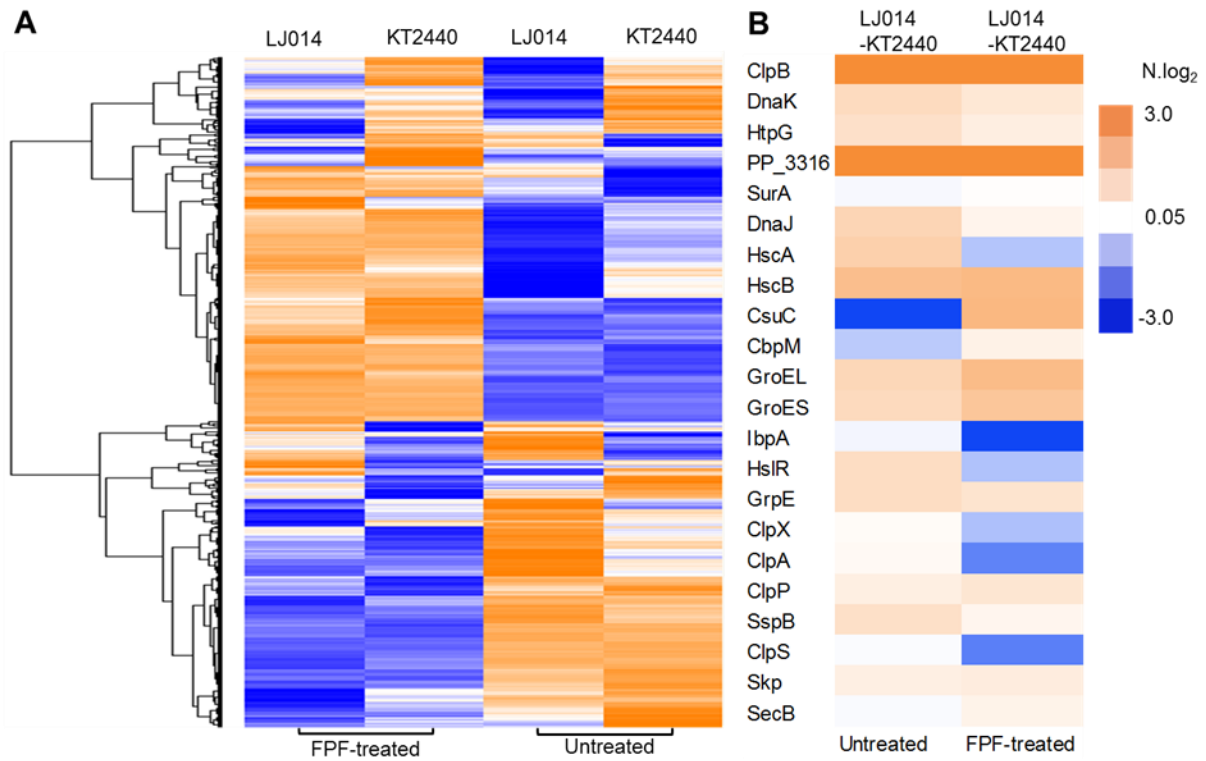


Figure S8. (A) Heat map of global proteomics profiles of the LJ014 and the KT2440 strains in M9 medium containing 20 mM glucose with or without 0.5% (v/v) FPF (B) Heat map of the N. log₂ values of chaperone proteins between the LJ014 and the KT2440 strain in M9 medium containing 20 mM glucose with or without 0.5% (v/v) FPF. FPF: fast pyrolysis with fractionation.

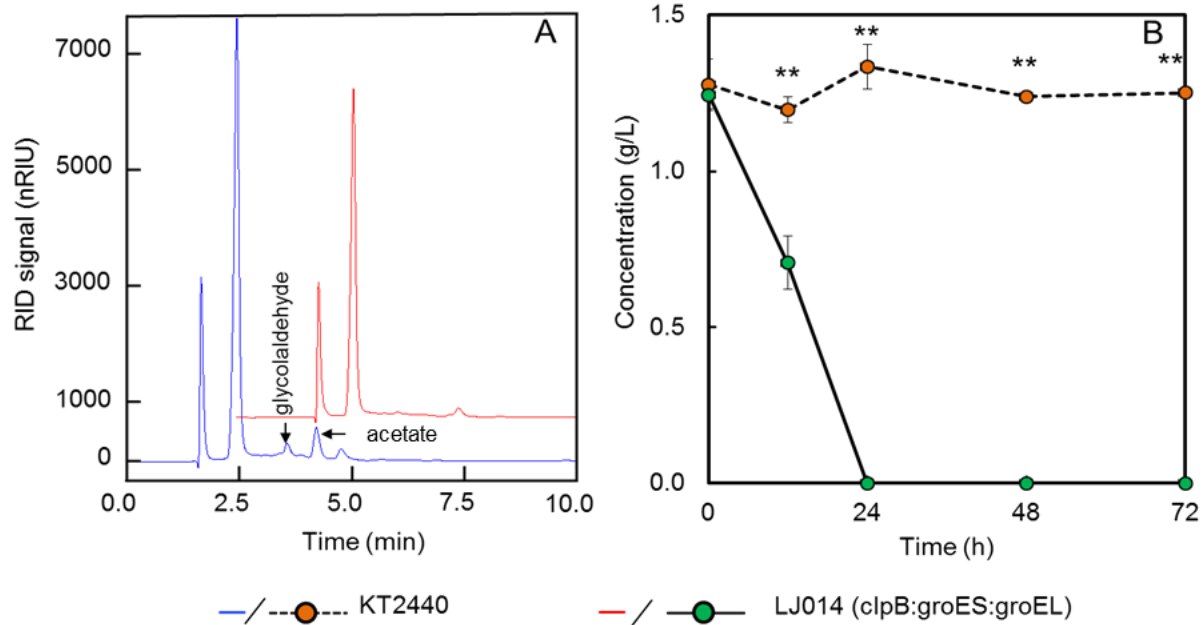


Figure S9. Consumption of acetate in FPF by LJ014 strain (A) HPLC chromatogram of media containing FPF as a sole carbon source (1% v/v) after 48 h of cultivation of KT2440 or LJ014. (B) Time course of acetate consumption of KT2440 and LJ014. The level of statistical significance is indicated for differences between the two strains (** $p < 0.01$). RID: refractive index detector, FPF: fast pyrolysis with fractionation.

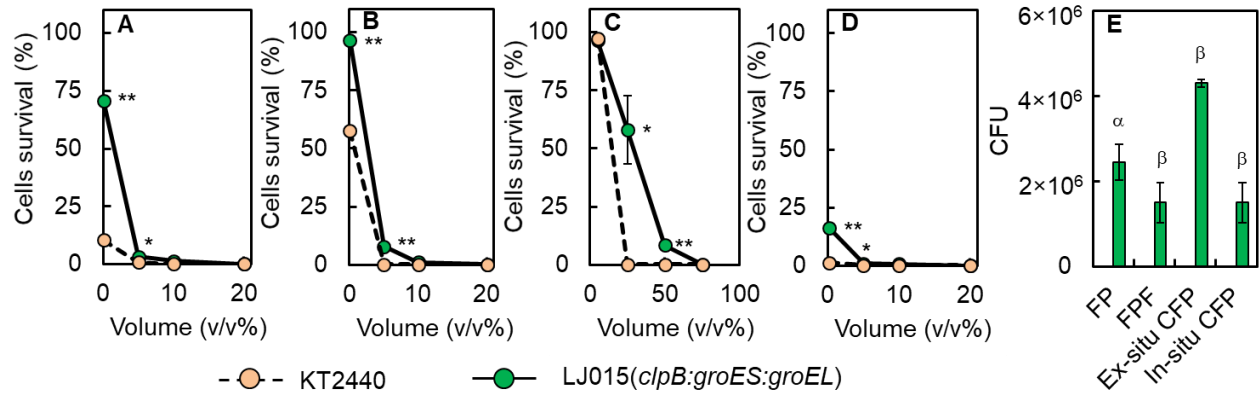


Figure S10. Cells survival at different concentrations of TC wastewater streams. (A) FP, (B) FPF, (C) *in-situ* CFC, (D) *ex-situ* CFP, and (E) CFU at maximum tolerable concentration (v/v%). The level of statistical significance is indicated for differences between the two strains (* $p < 0.05$, ** $p < 0.01$). Bars labeled with different symbols (α and β) indicate statistical significance in the differences in growth of rates s in different TC wastewater streams ($p < 0.05$; one-way ANOVA followed by Tukey's post hoc honest significance difference test). Bars labeled with the same symbol indicate no statistically significant difference ($p > 0.05$; one-way ANOVA followed by Tukey's post hoc honest significance difference test). TC: thermochemical: FP: fast pyrolysis, FPF: fast pyrolysis with fractionation, CFP: catalytic fast pyrolysis, ANOVA: analysis of variance.

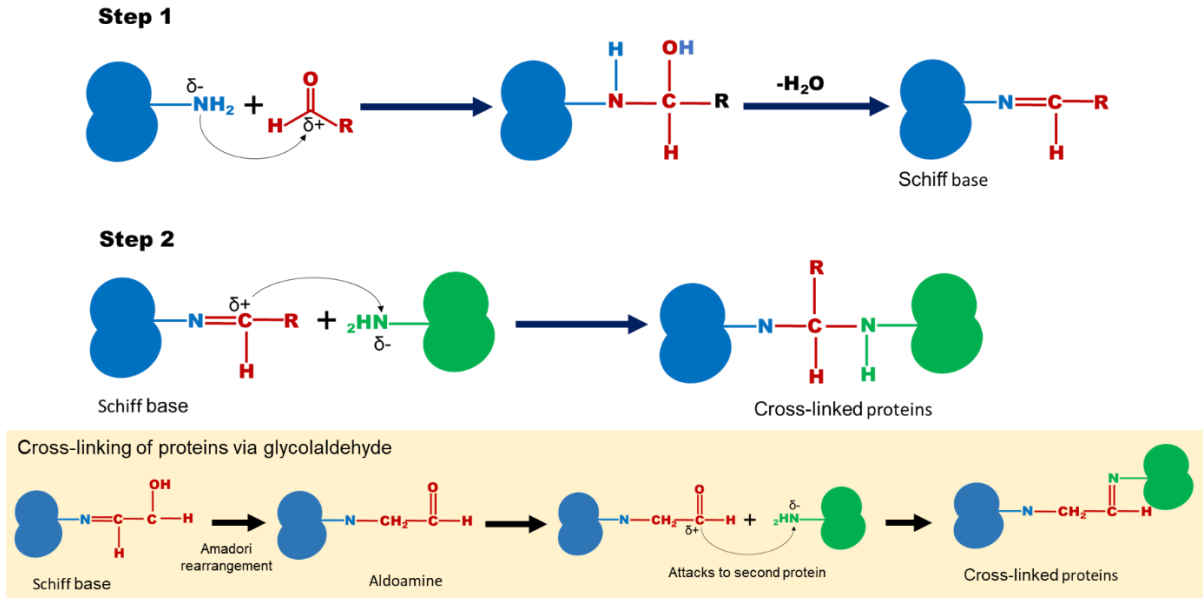


Figure S11: Schematic illustration of formation of cross-linked protein by aldehydes. Step 1: formation of Schiff with aldehydes, Step 2: Schiff base attacks to amino group of another protein and forms a cross-linked proteins. The formed Schiff base with α -hydroxyaldehydes such as glycolaldehyde undergoes Amadori rearrangement to make an aldoamine, and attacks to nitrogen atoms of the amino base of another protein.

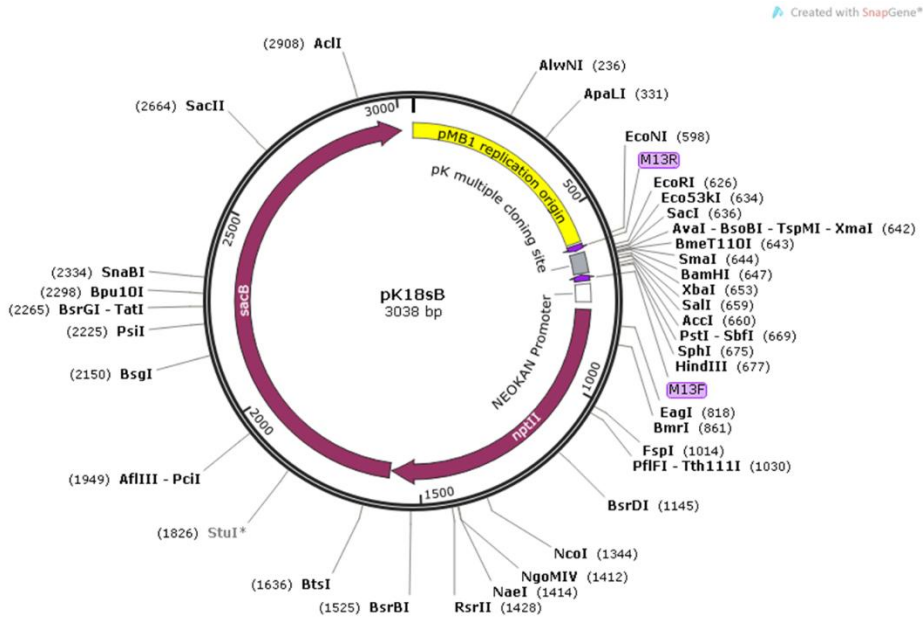


Figure S12. Map of the pK18sB vector, a smaller derivative of *sacB*-based genome integration vector pK18mobsacB. This plasmid is unable to replicate in *P. putida* and contains kanamycin antibiotic resistance gene to select for integration of the plasmid into the genome and *sacB* to counter select for recombination of the plasmid out of the genome. The sequence of this plasmid has been deposited at Genbank, accession number MH166772.

Table S1. Chemical composition of FPF

	Compound	Concentration (g/L)	Concentration (M)	Weight %	Carbon weight (g/L)	Carbon weight %
Acids	Acetic acid ^{a**, 8}	114.64	1.9091	33.81	45.86	31.05
	Formic acid ^{a**, 9}	60.37	1.3117	17.81	15.75	10.67
	Propionic acid ^{a**, 10}	3.4	0.0459	1.00	1.65	1.12
	Butanoic acid ^a	1.64	0.0186	0.48	0.89	0.61
	Crotonic acid	0.98	0.0114	0.29	0.55	0.37
	Acrylic acid ^a	7.5	0.1041	2.21	3.75	2.54
	Pentanoic acid ^a	0.11	0.0011	0.03	0.06	0.04
	Itaconic acid ^a	7.13	0.0548	2.10	3.29	2.23
Aldehydes	Glycolaldehyde ^{a*, 11}	51.46	0.8570	15.18	20.58	13.94
	Acetaldehyde ^{a**, this study}	4.36	0.0990	1.29	2.38	1.61
	Furfural ^{a*, 12}	10.7	0.1114	3.16	6.69	4.53
	Crotonaldehyde ^a	4.38	0.0625	1.29	3.00	2.03
	5-Methylfurfural ^a	1.05	0.0095	0.31	0.69	0.47
	5-(Hydroxymethyl)furfural ^{a*, 12}	0.54	0.0043	0.16	0.31	0.21
	2-Methyl-2-butenal ^a	0.05	0.0006	0.01	0.04	0.02
	3-Furaldehyde ^a	0.28	0.0029	0.08	0.18	0.12
	Vanillin ^{a**, 13}	1.52	0.0100	0.45	0.96	0.65
Ketones	Acetone ^a	6.01	0.1035	1.77	3.73	2.52
	Acetol ^a	6.89	0.0930	2.03	3.35	2.27
	2-Oxobutanol ^a	3.92	0.0445	1.16	2.14	1.45
	Acetoin	0.3	0.0034	0.09	0.16	0.11
	Cyclopentenone ^a	4.08	0.0497	1.20	2.98	2.02
	Cyclotene ^a	2.92	0.0260	0.86	1.88	1.27
	2-methylcyclopentenone ^a	1.38	0.0144	0.41	1.03	0.70
	1-Methyl-1-cyclopenten-3-one	0.85	0.0088	0.25	0.64	0.43
	2,3-Dimethyl-1-cyclopenten-1-one	0.43	0.0039	0.13	0.33	0.22
	Methyl vinyl ketone	0.09	0.0013	0.03	0.06	0.04
	Butyrolactone ^a	1.11	0.0129	0.33	0.62	0.42
	Methylpropyl ketone	0.67	0.0078	0.20	0.47	0.32
	Cyclopentanone	0.39	0.0046	0.12	0.28	0.19

	1,2-Cyclopentanedione	0.2	0.0020	0.06	0.12	0.08
	Maple lactone	0.07	0.0006	0.02	0.04	0.03
	1,4-Cyclohexanedione	0.15	0.0013	0.04	0.10	0.07
	Biacetyl	0.51	0.0059	0.15	0.28	0.19
	Acetylpropionyl	0.2	0.0020	0.06	0.12	0.08
	2-Acetylfuran	0.35	0.0032	0.10	0.23	0.16
	Maltol	0.29	0.0023	0.09	0.17	0.11
	2(5H)-Furanone ^a	24.72	0.2940	7.29	14.13	9.57
	3-Methyl-2(5H)-furanone	0.95	0.0097	0.28	0.58	0.39
	4-Methyl-2(5H)-furanone	0.33	0.0034	0.10	0.20	0.14
	5-Methyl-2(5H)-furanone	0.56	0.0057	0.17	0.34	0.23
<i>Phenolics</i>	Phenol ^a	1.39	0.0148	0.41	1.06	0.72
	Guaiacol ^a	1.66	0.0134	0.49	1.12	0.76
	Syringol ^a	0.56	0.0036	0.17	0.35	0.24
	o-Cresol ^a	0.6	0.0055	0.18	0.47	0.32
	m-Cresol ^a	0.45	0.0042	0.13	0.35	0.24
	p-Cresol ^a	0.45	0.0042	0.13	0.35	0.24
	Creosol ^a	0.86	0.0062	0.25	0.60	0.40
	4-propylguaiacol	0.03	0.0002	0.01	0.02	0.01
	Catechol ^{a**, 13}	0.34	0.0031	0.10	0.22	0.15
	4-Ethylguaiacol	0.29	0.0019	0.09	0.21	0.14
	4-Vinylguaiacol	0.02	0.0001	0.01	0.01	0.01
	2,3-Xylenol	0.02	0.0002	0.01	0.02	0.01
	1,3,5-Xylenol	0.01	0.0001	0.00	0.01	0.01
	2,6-Xylenol	0.07	0.0006	0.02	0.06	0.04
	2,5-Xylenol ^a	0.34	0.0028	0.10	0.27	0.18
	Trans-isoeugenol	0.05	0.0003	0.01	0.04	0.02
	Eugenol	0.18	0.0011	0.05	0.13	0.09
	2,5-Dimethoxytetrahydrofuran	0.11	0.0008	0.03	0.06	0.04
	2-Ethylphenol	0.03	0.0002	0.01	0.02	0.02
	2,3,5-Trimethylphenol	0.06	0.0004	0.02	0.05	0.03
	2,3,4-Trihydroxybenzoic acid	0.14	0.0008	0.04	0.07	0.05
	3,4,5-Trihydroxybenzoic acid	0.18	0.0011	0.05	0.09	0.06

	Apocynin	0.02	0.0001	0.01	0.01	0.01
Sugars	Levoglucofan	3.68	0.0202	1.09	1.46	0.99
Alcohol	1-Propanol	0.04	0.0007	0.01	0.02	0.02

^a Compounds included in the synthetic medium

^{**} Compounds can be completely metabolized by *P. putida* KT2440, as described in published literature

^{*} Compounds can be partially metabolized by *P. putida* KT2440, as described in published literature

Weight % was calculated based on the ratio of weight of particular compound and total weight of compounds.

Carbon % was calculated based on the ratio of carbon weight of particular compound and total carbon weight of compounds.

Table S2. EC₅₀ value of the most abundant compounds found in the thermochemical wastewater streams on *P. putida* KT2440

Category	Compound	EC ₅₀ (mM)	SEM
Aldehydes	Glycolaldehyde	2.14	0.42
	Acetaldehyde	16.19	1.81
	Furfural	20.97	3.98
	Crotonaldehyde	17.37	2.81
	5-methylfufaral	14.96	1.02
	5-HMF	14.33	1.39
	3-Furancarboxaldehyde	13.90	2.99
	Vanillin	6.34	0.04
	Glyoxal	3.50	0.28
	Formaldehyde	2.07	0.19
Ketones	Acetone	39.34	0.01
	Acetol	12.42	1.16
	2-Oxobutanol	27.75	0.61
	Methylolacetone	28.75	0.31
	Adipic ketone	9.80	1.24
	2-Butenolide	7.77	1.11
	2-Methyl-butenolide	5.02	0.52
Phenolics	Phenol	9.24	0.15
	Guaiacol	13.27	2.11
	Syringol	4.21	0.57
	<i>o</i> -Cresol	3.12	0.01
	<i>m</i> -Cresol	3.46	0.47
	<i>p</i> -Cresol	2.25	0.44
	Catechol	42.41	6.47
2,5-Xylenol	2.52	0.12	
Acids	Acetic acid	64.06	5.19
	Formic acid	258.41	15.19
	Propionic acid	22.44	1.33
	Butanoic acid	35.25	3.03
	Acrylic acid	11.68	0.46
	Itaconic acid	89.40	16.33

Table S3. Significantly upregulated genes in both GA and FPF-treated *P. putida* KT2440 cultures compared to control cultures.

Gene	Annotation	N. Log ₂ (GA) - N. Log ₂ (untreated)	N. Log ₂ (FPF-treated) - N. Log ₂ (untreated)
PP_1395	transcriptional regulator, AraC family	2.66	3.41
PP_1396	hypothetical protein	4.12	4.43
PP_1397	hypothetical protein	3.07	2.94
PP_2093	response regulator receiver and ANTAR domain protein	2.16	2.21
PP_2213	acyl-CoA ligase	2.28	2.27
PP_2425	transcriptional regulator, AraC family	5.67	4.96
PP_2426	D-isomer specific 2-hydroxyacid dehydrogenase family protein	7.85	6.12
PP_2427	hypothetical protein	3.07	2.02
PP_2476	alcohol dehydrogenase, zinc-containing	3.56	2.19
PP_2647	major facilitator family transporter	6.11	3.59
PP_3425	multidrug efflux RND membrane fusion protein MexE	7.01	4.80
PP_3426	multidrug efflux RND transporter MexF	6.51	4.11
PP_3427	multidrug efflux RND outer membrane protein OprN	6.58	4.68
PP_3519	lipoprotein, putative	4.31	2.31
PP_3621	isoquinoline 1-oxidoreductase, alpha subunit, putative	2.48	3.78
PP_3622	isoquinoline 1-oxidoreductase, beta subunit, putative	2.88	3.60
PP_3623	cytochrome c family protein	2.58	3.41
PP_3745	glycolate oxidase, subunit GlcD	3.77	3.66
PP_3747	glycolate oxidase, iron-sulfur subunit	3.33	3.96
PP_3748	glcG protein	2.08	2.07
PP_3770	hypothetical protein	7.87	4.66
PP_4087	hypothetical protein	3.22	2.25
PP_4858	hypothetical protein	6.97	4.67
PP_5287	hypothetical protein	2.35	2.33
PP_5390	hypothetical protein	2.07	2.26

Table S4. Gene ontologies enriched in differentially expressed genes identified by RNA seq analysis after FPF or glycolaldehyde-treatment.

	FPF-treated vs untreated	GA-treated vs untreated
Upregulated genes	<ul style="list-style-type: none"> No GO enrichment 	<ul style="list-style-type: none"> Structural constituent of ribosome Iron ion binding Siderophore transport
Downregulated genes	<ul style="list-style-type: none"> Alginate biosynthesis process Proton-transporting ATP synthase complex, catalytic core F(1) Plasma membrane ATP synthesis coupled proton transport Succinate-CoA ligase (ADP-forming) activity Proton-transporting ATP synthase activity, Rotational mechanism Ligase activity, forming nitrogen-metal bonds, forming coordination complexes 	<ul style="list-style-type: none"> No GO enrichment

Table S5. Gene ontologies enriched in differentially expressed proteins

	KT2440(FPF-treated) vs KT2440(untreated)	LJ014 (untreated) vs KT2440(untreated)	LJ014(FPF-treated) vs KT2440(FPF-treated)
Higher expression	<ul style="list-style-type: none"> Iron ion binding Gluconate dehydrogenase activity Benzoate 1,2-dioxygenase activity 	<ul style="list-style-type: none"> No GO enrichment 	<ul style="list-style-type: none"> Siderophore transport Receptor activity Iron ion binding
Lower expression	<ul style="list-style-type: none"> Oxidation-reduction process Oxidoreductase activity, Acting on CH-OH group of donors Flavin adenine dinucleotide binding Acetate-CoA ligase activity Acyl-CoA dehydrogenase activity Acetyl-CoA activity Acyltransferase activity Metal ion transport Sarcosine oxidase activity 	<ul style="list-style-type: none"> No GO enrichment 	<ul style="list-style-type: none"> No GO enrichment

Table S6. Comparison of the most highly expressed RNAs and protein expression in *putida* KT2440 upon FPF treatment

Gene	Description	RNA-seq	Proteomics	log ₂
PP_2425	transcriptional regulator, AraC family	3	3	3
PP_3427	multidrug efflux RND outer membrane protein OprN	2	2	2
PP_2791	aminoglycoside phosphotransferase	1	1	1
PP_3425	multidrug efflux RND membrane fusion protein MexE	0	0	0
PP_3426	multidrug efflux RND transporter MexF	-1	-1	-1
PP_3745	glycolate oxidase, subunit GlcD	-2	-2	-2
PP_1395	transcriptional regulator, AraC family	-3	-3	-3
PP_2793	acyl-CoA dehydrogenase family protein			
PP_3171	hypothetical protein			
PP_2792	hypothetical protein			
PP_2795	acyl-CoA synthase			
PP_1397	hypothetical protein			
PP_2797	acetate permease			
PP_0057	major facilitator family transporter			
PP_3746	glycolate oxidase, subunit GlcE			
PP_2213	acyl-CoA ligase			
PP_2476	alcohol dehydrogenase, zinc-containing			
PP_3332	cytochrome c-type protein			
PP_2727	C-factor, putative			
PP_1427	RNA polymerase, sigma-24 subunit, RpoE			
PP_1188	C4-dicarboxylate transport protein			
PP_1418	tricarboxylate transport protein TctC, putative			
PP_2475	transcriptional regulator, TetR family			
PP_2681	pyrroloquinoline quinone biosynthesis protein PqqD			
PP_2827	alcohol dehydrogenase, zinc-containing			
PP_1829	hydrolase, alpha/beta fold family			
PP_1964	deoxynucleotide monophosphate kinase, putative			
PP_3748	glcG protein			
PP_0837	hypothetical protein			
PP_1148	hypothetical protein			
PP_1750	asparagine synthase (glutamine-hydrolysing)			
PP_3743	hypothetical protein			
PP_4281	guanine deaminase (EC 3.5.4.3)			
PP_2794	oxidoreductase, short chain dehydrogenase/reductase family			
PP_2645	magnesium-translocating P-type ATPase			
PP_4738	hypothetical protein			
PP_2059	hypothetical protein			
PP_4491	pterin-4-alpha-carbinolamine dehydratase			
PP_0740	transcriptional regulator, MerR family			
PP_4264	coproporphyrinogen III oxidase, anaerobic			
PP_1254	xenobiotic reductase A			

PP_1930	transcriptional regulator, ArsR family	
PP_3764	porin, putative	
PP_5391	hypothetical protein	
PP_2495	hypothetical protein	
PP_1323	phosphoheptose isomerase	
PP_3929	hypothetical protein	
PP_1503	hypothetical protein	
PP_0149	hypothetical protein	
PP_2099	hypothetical protein	
PP_1357	hypothetical protein	
PP_1387	transcriptional regulator, TetR family	
PP_3631	hypothetical protein	
PP_0333	hypothetical protein	
PP_4297	glyoxylate carboligase	
PP_3610	hypothetical protein	
PP_4288	ureidoglycolate hydrolase	
PP_1300	amino acid ABC transporter ATP-binding protein, PAAT family	
PP_3223	ABC transporter, periplasmic binding protein	
PP_2270	DNA primase/helicase	

Table S7. Proteins more highly expressed in LJ014 relative to KT2440 when treated with 0.05% FPF (V/V)

Protein	Description	N. Log ₂
PP_1315	50S ribosomal protein L13 RplM	1.26
PP_3316	Putative Chaperone-associated ATPase	4.14
PP_1911	50S ribosomal protein L32 RpmF	1.19
PP_0938	Uncharacterized protein	1.81
PP_4809	Ribosomal silencing factor RsfS	2.84
PP_3095	Protein ClpV1	3.27
PP_4007	Translation initiation factor IF-1 InfA	2.02
PP_3332	Putative cytochrome c-type protein	1.07
PP_2468	50S ribosomal protein L20 RplT	1.38
PP_1352	UPF0234 protein	1.13
PP_3248	Dyp-type peroxidase family protein	1.02
PP_5171	Sulfate ABC transporter Sbp-II	1.36
PP_2698	5-methyltetrahydropteroyltriglutamate-homocysteine methyltransferase metE	1.61
PP_0472	50S ribosomal protein L30 RpmD	1.36
PP_3785	Uncharacterized protein	1.02
PP_1765	Ubiquinone biosynthesis O-methyltransferase UbiG	1.77
PP_4375	Flagellar protein FliS	1.61
PP_3722	Alanine racemase Alr	2.02
PP_2008	2,4-dienoyl-CoA reductase OS=Pseudomonas putida FadH	4.78
PP_5141	Thymidylate synthase ThyA	1.79
PP_3335	Uncharacterized protein	3.15

PP_4770	Uncharacterized protein	1.51
PP_5103	tRNA (guanine-N (7)-)-methyltransferase TrmB	1.88
PP_0046	Tyrosine-specific outer membrane porin D OpdT-I	1.13
PP_1673	Hydrogenobyrrinate a,c-diamide synthase CobB	1.08
PP_4717	Dihydropteroate synthase FolP	1.21
PP_4613	Outer membrane ferric citrate porin FecA	1.95
PP_0267	Putative Outer membrane ferric siderophore receptor	2.73
PP_4362	Uncharacterized protein	1.79
PP_5025	Glucans biosynthesis glucosyltransferase OpgH	1.43
PP_3321	Uncharacterized protein	2.27
PP_1619	tRNA pseudouridine synthase TruD	1.11
PP_1757	DNA-binding transcriptional dual regulator BolA	1.19
PP_4601	Transcriptional regulator, LysR family	1.72
PP_3120	Methylglyoxal reductase YeaE	1.50
PP_2132	Universal stress protein	4.08
PP_0845	Co-chaperone protein HscB	1.08
PP_4144	Hydroxyacylglutathione hydrolase GloB	1.01
PP_5097	Homoserine O-acetyltransferase MetX	1.79
PP_3958	Na ⁺ /H ⁺ antiporter NhaA 2	1.27
PP_0354	CBS domain protein	1.01
PP_0529	Exodeoxyribonuclease 7 small subunit XseB	1.31
PP_5361	47 kDa protein	2.20
PP_3828	Molybdate-binding periplasmic protein ModA	1.13
PP_0879	Dipeptide ABC transporter-putative ATP binding subunit DppD PE	1.19
PP_3948	Nicotinate dehydrogenase subunit B NicB	2.48
PP_5212	Oxidoreductase, iron-sulfur-binding	1.06
PP_3654	Leucine-responsive regulatory protein	1.92
PP_0341	ADP-heptose:LPS heptosyltransferase II WaaF	2.07
PP_0962	Toluene-tolerance protein Ttg2E	2.05
PP_2668	ABC efflux transporter, ATP-binding protein	1.06
PP_1209	Cold-shock protein	1.03
PP_2440	Alkyl hydroperoxide reductase subunit F AhpF	1.36
PP_4657	Zinc metalloprotease YpfJ	1.32
PP_5045	tRNA sulfurtransferase ThiI	1.42
PP_3056	Putative Pyocin R2_PP, tail fiber protein	2.61
PP_2126	DNA-binding response regulator, LuxR family	4.58
PP_2036	Putative 4-hydroxy-tetrahydrodipicolinate synthase	1.50
PP_4066	Methylglutaconyl-CoA hydratase LiuC	1.23
PP_1597	1-deoxy-D-xylulose 5-phosphate reductoisomerase Dxr	4.35
PP_4648	Ribosomal RNA large subunit methyltransferase G RlmG	1.02
PP_0029	Two component heavy metal response regulator CzcR-I	1.50
PP_5054	Glutaredoxin 3 GrxC	1.31
PP_5388	Probable exported copper efflux protein CusF	1.59
PP_5314	Rubredoxin-NAD ⁺ reductase AlkT	2.01

PP_5068	UPF0061 protein	1.47
PP_1936	Uncharacterized protein	3.17
PP_3964	Transposase	5.50
PP_1290	Polysaccharide deacetylase family protein	1.06
PP_5431	Uncharacterized protein	1.62
PP_0400	Protein ApaG	1.66
PP_0242	Transcriptional regulator, TetR	1.29
PP_4285	5-hydroxyisourate hydrolase PucM	1.06
PP_0342	ADP-heptose:LPS heptosyltransferase I WaaC	1.08
PP_4814	ATP-dependent protease La domain protein	1.11
PP_2485	Uncharacterized protein	3.43
PP_4943	Putative Glycosyl transferase	1.06
PP_0052	Beta-lactamase domain protein, putative hydrolase	1.90
PP_3575	Outer membrane ferric siderophore receptor	3.87
PP_1395	Transcriptional regulator, AraC	1.00
PP_2696	DNA-binding transcriptional regulator, homocysteine-binding MetR-II	1.06
PP_2447	Uncharacterized protein	1.78
PP_3104	Uncharacterized protein	1.88
PP_0286	Adenine glycosylase MutY	1.19
PP_3989	DNA-cytosine methyltransferase	2.71
PP_5099	Uncharacterized protein	1.43
PP_2079	Uncharacterized protein	1.10
PP_0237	Aliphatic sulfonate ABC transporter-periplasmic binding protein / transport of isethionate SsuA	2.35
PP_1262	LysR family transcriptional regulator	1.18
PP_3509	Glyoxalase family protein	1.34
PP_5274	Uncharacterized protein	1.45
PP_3446	L-threonine dehydratase IlvA-I	1.11
PP_1144	Uncharacterized protein	2.11
PP_5253	Arylesterase OS=Pseudomonas putida	1.38
PP_1128	OmpA family protein	2.93
PP_3779	Transcriptional regulator, LysR family	2.78
PP_3155	Putative Outer membrane ferric siderophore receptor	2.78
PP_3008	Uncharacterized protein	2.65
PP_1492	Sensor histidine kinase/response regulator	1.13
PP_2016	Uncharacterized protein	1.16
PP_2379	Putative cytochrome oxidase biogenesis protein	1.21
PP_1073	Glycerol-3-phosphate dehydrogenase GlpD	2.01
PP_0820	GCN5-related N-acetyltransferase	1.45
PP_4745	Transposase	1.12
PP_1413	Uracil-DNA glycosylase Ung	2.61
PP_2414	Uncharacterized protein	1.29
PP_5618	Putative Cro/CI transcriptional regulator	1.71
PP_3573	Putative Monooxygenase	3.99
PP_0307	Uncharacterized protein	1.59

PP_5022	Glutamine transport ATP-binding protein GlnQ	1.09
PP_1221	Colicin S4 and filamentous phage transport system TolA	1.97
PP_1677	Cobyric acid synthase CobQ	2.66
PP_2650	Putative 4-hydroxybutyrate dehydrogenase Gbd	3.08
PP_2387	Uncharacterized protein	3.15
PP_4042	Glucose-6-phosphate 1-dehydrogenase ZwfB	1.25
PP_1672	Cob(I)alamin adenosyltransferase/cobinamide ATP-dependent adenosyltransferase	1.90
PP_3139	Glycosyl transferase, group 1 family protein	1.67
PP_0500	dTDP-4-rhamnose reductase-related protein	1.55
PP_3231	Uncharacterized protein	1.18
PP_5002	Uncharacterized protein	1.06
PP_1078	Putative ABC transporter, ATP-binding protein	1.89
PP_4674	RecBCD enzyme subunit RecC	1.28
PP_1516	RND membrane fusion protein	1.16
PP_3596	D-lysine oxidase AmaD	1.16
PP_3795	Uncharacterized protein	1.55
PP_4334	ParA family protein	1.64
PP_4761	Hydrolase, haloacid dehalogenase-like family	2.11
PP_1695	Putative Sodium-solute symporter/sensory box histidine kinase/response regulator	2.93
PP_2912	Uncharacterized protein	1.94
PP_3254	Putative Nucleosidase	1.35
PP_3067	Uncharacterized protein	1.24
PP_2443	Serine/threonine transporter SstT	1.22
PP_2836	Putative 2-keto-3-deoxyxylonate dehydratase	2.44
PP_2198	Aldose sugar dehydrogenase YliI	1.52
PP_0495	Type 1 L-asparaginase AnsA	1.03
PP_4171	Uncharacterized protein	1.11
PP_0136	Uncharacterized protein	1.13
PP_0976	Ribosomal RNA large subunit methyltransferase RlmF	1.23
PP_5101	Coproporphyrinogen/heterocyclic compound oxidase (Aerobic) yggW	1.72
PP_2005	Uncharacterized protein	1.31
PP_0861	Outer membrane ferric siderophore receptor	4.30
PP_3367	Uncharacterized protein	1.59
PP_3811	Transcriptional regulator, LysR family	2.22
PP_3116	LexA repressor 2	2.18
PP_2891	Acetyltransferase, GNAT family	1.41
PP_3364	Response regulator	1.29
PP_3563	Uncharacterized protein	1.28
PP_3191	Putative threonine ammonia-lyase / dehydratase	2.49
PP_0008	Ribonuclease P protein component RnpA	1.17
PP_0619	Branched-chain amino acid ABC transporter, periplasmic amino acid-binding protein	1.72
PP_3671	Oxidoreductase, aldo/keto reductase family	1.04
PP_3421	Sensor histidine kinase	1.21
PP_0076	Putative choline betaine-binding protein	1.25

PP_5133	Uncharacterized protein	1.36
PP_1105	Putative DNA ligase, ATP-dependent	1.10
PP_4336	Flagellar motor rotation protein	1.08
PP_0936	Maf-like protein PP_0936 Maf-1	1.50
PP_4831	Cobalt-precorrin-5B C(1)-methyltransferase	1.39
PP_4738	Uncharacterized protein	1.46
PP_4683	Penicillin-binding protein 1B	1.12
PP_0238	Alkanesulfonate monooxygenase	2.91
PP_1881	Uncharacterized protein	1.34
PP_5464	Uncharacterized protein	1.04
PP_1028	Transcriptional regulator, LysR family	1.05
PP_0350	Outer membrane ferrichrome-iron receptor	1.33
PP_3757	Chemotaxis protein CheY	1.47
PP_5221	UPF0178 protein PP_5221	1.28
PP_1788	Uncharacterized protein	1.03
PP_4109	Uncharacterized protein	3.34
PP_4405	Sensory box protein	1.23
PP_0561	Thiol:disulfide interchange protein DsbD	1.16
PP_2682	Fe-containing alcohol dehydrogenase YiaY	1.45
PP_3985	Transposase	1.75
PP_2052	Putative bifunctional enzyme: sugar-phosphatase/mannitol-1-phosphate 5-dehydrogenase	1.26
PP_5169	Sulfate ABC transporter, inner membrane subunit CysW	1.80
PP_1824	Smr domain protein	2.02
PP_4622	Hmg transcriptional repressor	1.54
PP_0224	Monooxygenase, DszC family	4.07
PP_3387	Uncharacterized protein	2.09
PP_0563	Response regulator	2.07
PP_5308	Protein TonB	1.76
PP_2727	Putative C-factor	1.26
PP_0180	Putative cytochrome c family protein	1.16
PP_4555	Uncharacterized protein	1.85
PP_2495	Uncharacterized protein	2.05
PP_2578	Uncharacterized protein	1.45
PP_4584	Putative endonuclease YajD	1.10
PP_1921	Uncharacterized protein	1.14
PP_0868	ABC transporter ATP-binding subunit	2.32
PP_2540	Oxidoreductase, short-chain dehydrogenase/reductase family	1.25
PP_3510	Uncharacterized protein	1.37
PP_4333	CheW domain protein	1.22
PP_4855	Osmotically-inducible lipoprotein OsmE	1.43
PP_1424	Uncharacterized protein PP_1424	1.00
PP_5140	Transcriptional regulator, MerR family	1.29
PP_2566	Uncharacterized protein	1.74
PP_3810	Uncharacterized protein	1.40

PP_2877	Putative osmotic pressure-regulated transporter YyfeH	1.27
PP_4032	Putative Outer membrane lipoprotein Blc	2.89
PP_1350	Sensory box histidine kinase/response regulator	4.26
PP_3142	Putative Sugar transferase	1.70
PP_4294	Conserved inner membrane protein YyedI	2.14
PP_0944	Fumarate hydratase class II FumC-I	1.14
PP_1005	Heme oxygenase HemO	1.26
PP_5659	Uncharacterized protein	1.24
PP_3753	Transcriptional regulator, AraC family	2.14

Table S8. Strain used for the study

Strain ID	Genotype	Description of strain
KT2440	<i>P. putida</i> KT2440	Wild-type <i>P. putida</i> KT2440 (ATCC 47054)
EM42	<i>P. putida</i> KT2440 Δ prophage1-4 Δ flagellum Δ endA-1 Δ endA-2 Δ Tn7 Δ hsdRMS Δ Tn4652	Genome reduced strain derived from <i>P. putida</i> KT2440 obtained from Victor de Lorenzo's laboratory (Centro Nacional de Biotecnología (CNB-CSIC), Madrid, Spain) ¹⁴
LJ001	KT2440 + pBTL-2	KT2440 containing the empty control plasmid (pBTL-2)
LJ002	KT2440 + pBTL-2- <i>clpB</i>	KT2440 containing plasmid pLJ001 for overexpression of <i>groES</i>
LJ003	KT2440 + pBTL-2- <i>groES</i>	KT2440 containing plasmid pLJ002 of overexpression of <i>groES</i>
LJ004	KT2440 + pBTL-2- <i>groEL</i>	KT2440 containing plasmid pLJ003 of overexpression of <i>groEL</i>
LJ005	KT2440 + pBTL-2- <i>groES-groEL</i>	KT2440 containing plasmid pLJ004 of overexpression of <i>groES</i> and <i>groEL</i>
LJ006	KT2440 + pBTL-2- <i>clpB-groES-groEL</i>	KT2440 containing plasmid pLJ005 of overexpression of <i>groES</i> , <i>groEL</i> , and <i>clpB</i>
LJ007	KT2440 + pBTL-2- <i>dnaJ</i>	KT2440 containing plasmid pLJ006 of overexpression of <i>dnaJ</i>
LJ008	KT2440 + pBTL-2- <i>dnaK</i>	KT2440 containing plasmid pLJ007 of overexpression of <i>dnaK</i>
LJ009	KT2440 + pBTL-2- <i>grpE</i>	KT2440 containing plasmid pLJ008 of overexpression of <i>grpE</i>
LJ010	KT2440 + pBTL-2- <i>dnaJ-dnaK-grpE</i>	KT2440 containing plasmid pLJ009 of overexpression of <i>dnaJ</i> , <i>dnaK</i> , and <i>grpE</i>
LJ011	KT2440 + pBTL-2- <i>dnaJ-dnaK-grpE-clpB</i>	KT2440 containing plasmid pLJ010 of overexpression of <i>dnaJ</i> , <i>dnaK</i> , <i>grpE</i> , and <i>clpB</i>
LJ012	KT2440 + pBTL-2- <i>dnaJ-dnaK-grpE-groES-groEL</i>	KT2440 containing plasmid pLJ011 of overexpression of <i>dnaJ</i> , <i>dnaK</i> , <i>grpE</i> , <i>groES</i> , and <i>groEL</i>
LJ013	KT2440 + pBTL-2- <i>dnaJ-dnaK-grpE-clpB-groES-groEL</i>	KT2440 containing plasmid pLJ012 of overexpression of <i>dnaJ</i> , <i>dnaK</i> , <i>grpE</i> , <i>clpB</i> , <i>groES</i> , and <i>groEL</i>
LJ014	KT2440 PP_1584::Ptac:: <i>clpB-groES-groEL</i>	KT2440 with the <i>clpB-groES-groEL</i> chaperone expression cassette integrated within the intergenic region between PP_1584 and PP_1585
LJ015	EM42 PP_1584::Ptac:: <i>clpB-groES-groEL</i>	EM42 with the <i>clpB-groES-groEL</i> chaperone expression cassette integrated within the intergenic region between PP_1584 and PP_1585

Table S9. Thermochemical pyrolysis aqueous waste streams used in this study

Process	Abbreviation	Derived from	Source
Fast pyrolysis	FP	Pine	National Renewable Energy Laboratory
Fast pyrolysis with fractionation	FPF	Pine: 5 th fraction	Iowa State University
<i>in situ</i> catalytic fast pyrolysis	<i>in situ</i> CFP	Pine	RTI international
Ex situ catalytic fast pyrolysis	<i>ex situ</i> CFP	Pine: Davison circulating riser reactor with Ecat catalysis	National Renewable Energy Laboratory

Chemical compositions of these streams are reported in Black et al., 2016 and Starace et al., 2017.^{15,16}

Table S10. Primers used in construction of plasmids

Primer	Sequence [5'-3']
oLJ001	GGAATTGTGAGCGGATAACAATTTACACTTCCGACCTGCCCTTTAAAGGAAGGTACAC
oLJ002	AATTGTGGTTTTTCATAGCCCCGCAAACGCGGGG
oLJ003	CGCGTTTTCGCGGGGCTATGAAAACCAACAATTTGG
oLJ006	CGCTGGAGTCTGAGGCTCGTCCTGAATGATTTTTGATGGTGCAGGGGG
oLJ018	TGAGGCTCGTCCTGAATGATAGCCCCGCAAACGCGGGG
oLJ020	GCGGATAACAATTTACACTGCGGCCGCATGAAAACCAACAATTTGG
oLJ021	TGAGGCTCGTCCTGAATGATAAACTTTGGAGTAACGGG
oLJ022	GCGGATAACAATTTACACTGCGGCCGCTACTCCAAAGTTTTCAAGGATTAACG
oLJ050	GGAATTGTGAGCGGATAACAATTTACACTCTACCAAATTCAGTTTCGGGAGAG
oLJ051	CGCTGGAGTCTGAGGCTCGTCCTGAATGATCGGCCGACAACATGCAGG
oLJ065	GCGGATAACAATTTACACTAATTGCGCAGGAGAGACC
oLJ066	TGAGGCTCGTCCTGAATGATCCGAAGGATTTCAAGCCTTTTC
oLJ067	GCGGATAACAATTTACACTCAACAAGGTGCAAATGAC
oLJ068	TGAGGCTCGTCCTGAATGATCTGTTCTTGTGAGAGATCG
oLJ069	CCGAAACTTGCTGTTCTTGTGAGAGATCG
oLJ070	CAAGGAACAGCAAGTTTCGGGAGAGTTAACAT
oLJ071	CTGCGCAATTCATGCAGGGATTACTGCTTG
oLJ072	TCCCTGCATGAATTGCGCAGGAGAGACC
oLJ073	GCAGGTTCGGACCGAAGGATTTCAAGCCTTTTC
oLJ074	AATCCTTCGGTCCGACCTGCCCTTTAAAGGAAGGTACAC
oLJ075	TGGTTTTTCATCCGAAGGATTTCAAGCCTTTTC
oLJ076	AATCCTTCGGATGAAAACCAACAATTTGG
oLJ059	TGTGAGCGGATAACAATTTACACTTCCGACCTGCCCTTTAAAGGAAGGTACAC
oLJ060	GCCTCCGGTTCGGAGGCTTTTGACTATTTTGATGGTGCAGGGGG
oLJ144	GCGGGAGATCGACGCAAAAACCGCACCCAGGTG
oLJ145	GAAGATTTACGCAACAGTCAAAAAGCCTCCGGTTCG
oLJ146	GACATGATTACGAATTCGAGCTCGGTACCCTCGAGCCAGACCTACCCAGCG
oLJ147	TGGGTGCGGTTTTTTCGCTCGATCTCCCGCCGG
oLJ148	CGGAGGCTTTTGACTGTTGCGTAAATCTTCCCCAAAAT
oLJ149	CGGCCAGTGCCAAGCTTGCATGCCTGCAGGGCCGACCAGCTTCGACAG
oLJ154	CGCGGTATCCGCAACAACAA
oLJ155	ACGCATCGTTCATCAGTGCCT
oCJ382	AATTAACAGTTAAACAATAATCAGACCCCGTAGAAAAGATCAAAGGATCTTC
oCJ384	ATGATTGAACAAGATGGATTGCACGCAGG
oCJ385	AACTTTTTGATGTTTCATCGTCGCTCAGAAGAACTCGTCAAGAAGGCGATAGAAG
oCJ386	TTCTGAGCGACGATGAACATCAAAAAGTTTGCAAAAACAAGCAACAGTATTAACC
oCJ387	TACGGGGTCTGATTATTTGTTAACTGTTAATTGTCCTTGTTCAGGATGCTGTC
oCJ402	GGCGTTTTTTCATAGGCTCCGC

Table S11. Sequence of the synthetic DNA fragment used in construction of pK18sB

(5'-3')
TCAGGGGGGCGGAGCCTATGGAAAAACGCCTCACACAGGAAACAGCTATGACATGATTACGAATTCGAGCTCG GTACCCGGGGATCCTCTAGAGTCGACCTGCAGGCATGCAAGCTTGGCACTGGCCGTCGTTTTACAACGTCGTGA CCGGAATTGCCAGCTGGGGCGCCCTCTGGTAAGGTTGGGAAGCCCTGCAAACAGGATGAGGATCGTTTCGCATG ATTGAACAAGATGGATTGCACGCAGGT

Table S12. Plasmid construction details

Plasmid	Purpose	Construction detail
pK18sB (Genbank: MH166772)	Integration of genes into <i>P. putida</i> genome	From pK18mobsacB (GenBank: FJ437239.1), the pMB1 origin of replication was amplified with oCJ382/oCJ402 (595 bp), the nptII kanamycin resistance gene was amplified with oCJ384/oCJ385 (795 bp), and the sacB levan sucrose gene was amplified with oCJ386/oCJ387 (1,422 bp), and these products were assembled with a double-stranded DNA fragment synthesized by IDT containing the pK multiple cloning site and M13 F and M13 R primer binding sites.
pLJ001	Overexpressing <i>clpB</i>	A DNA fragment containing the <i>clpB</i> gene, including 30 base pairs upstream and 20 base pairs downstream, was amplified from <i>P. putida</i> KT2440 genomic DNA with primers oLJ001 (Fwd) and oLJ018 (Rev). This product was assembled into pBLT-2 digested with XbaI and EcoRV.
pLJ002	Overexpressing <i>groES</i>	A DNA fragment containing the <i>groES</i> gene, including 30 base pairs upstream and 20 base pairs downstream, was amplified from <i>P. putida</i> KT2440 genomic DNA with primers oLJ020 (Fwd) and oLJ021 (Rev). This product was assembled into pBLT-2 digested with XbaI and EcoRV.
pLJ003	Overexpressing <i>groEL</i>	A DNA fragment containing the <i>groEL</i> gene, including 30 base pairs upstream and 20 base pairs downstream, was amplified from <i>P. putida</i> KT2440 genomic DNA with primers oLJ022 (Fwd) and oLJ006 (Rev). This product was assembled into pBLT-2 digested with XbaI and EcoRV.
pLJ004	Overexpressing <i>groES</i> and <i>groEL</i>	A DNA fragment containing the <i>groES</i> and <i>groEL</i> genes, including 30 base pairs upstream and 20 base pairs downstream, was amplified from <i>P. putida</i> KT2440 genomic DNA with primers oLJ020 (Fwd) and oLJ006 (Rev). This product was assembled into pBLT-2 digested with XbaI and EcoRV.
pLJ005	Overexpressing <i>clpB</i> , <i>groES</i> and <i>groEL</i>	DNA fragments containing the <i>clpB</i> and <i>groES-groEL</i> genes, both with and 30 base pairs upstream and 20 base pairs downstream, were amplified from <i>P. putida</i> KT2440 genomic DNA with primers oLJ001 (Fwd) and oLJ002 (Rev), and oLJ003 (Fwd) and oLJ006, respectively. These products were assembled into pBLT-2 digested with XbaI and EcoRV.
pLJ006	Overexpressing <i>dnaJ</i>	A DNA fragment containing the <i>dnaJ</i> gene, including 30 base pairs upstream and 20 base pairs downstream, was amplified from <i>P. putida</i> KT2440 genomic DNA with primers oLJ067 (Fwd) and oLJ068. This product was assembled into pBLT-2 digested with XbaI and EcoRV.
pLJ007	Overexpressing <i>dnaK</i>	A DNA fragment containing the <i>dnaK</i> gene, including 30 base pairs upstream and 20 base pairs downstream, was amplified from <i>P. putida</i> KT2440 genomic DNA with primers oLJ050 (Fwd) and oLJ051. This product was assembled into pBLT-2 digested with XbaI and EcoRV.
pLJ008	Overexpressing <i>grpE</i>	A DNA fragment containing the <i>grpE</i> gene and 30 base pairs upstream and 20 base pairs downstream were amplified from <i>P. putida</i> KT2440 genomic DNA with primers oLJ065 (Fwd)

		and oLJ066. This product was assembled into pBLT-2 digested with XbaI and EcoRV.
pLJ009	Overexpressing <i>dnaJ</i> , <i>dnaK</i> , and <i>grpE</i>	DNA fragments containing the <i>dnaJ</i> , <i>dnaK</i> , and <i>grpE</i> genes, all with and 30 base pairs upstream and 20 base pairs downstream, were amplified from <i>P. putida</i> KT2440 genomic DNA with primers oLJ067 (Fwd) and oLJ069 (Rev), oLJ070 (Fwd) and oLJ071 (Rev), and oLJ072 (Fwd) and oLJ066 (Rev), respectively. These products were assembled into pBLT-2 digested with XbaI and EcoRV.
pLJ010	Overexpressing <i>dnaJ</i> , <i>dnaK</i> , <i>grpE</i> and <i>clpB</i>	A DNA fragment containing the <i>clpB</i> gene, including 30 base pairs upstream and 20 base pairs downstream, was amplified from <i>P. putida</i> KT2440 genomic DNA with primers oLJ074 (Fwd) and oLJ018 (Rev) and a fragment containing the <i>dnaJ</i> , <i>dnaK</i> , and <i>grpE</i> genes was amplified with primers oLJ067 (Fwd) and oLJ073 (Rev) using pLJ009 as a template. These products were assembled into pBLT-2 digested with XbaI and EcoRV.
pLJ011	Overexpressing <i>dnaJ</i> , <i>dnaK</i> , <i>grpE</i> , <i>groES</i> and <i>groEL</i>	A DNA fragment containing the <i>dnaJ</i> , <i>dnaK</i> , and <i>grpE</i> genes was amplified using pLJ009 as a template with primers oLJ067 (Fwd) and oLJ075 (Rev) and a DNA fragment containing the <i>groES</i> and <i>groEL</i> genes, including 30 base pairs upstream and 20 base pairs downstream, was amplified with primers oLJ076 (Fwd) and oLJ006 (Rev) from <i>P. putida</i> KT2440 genomic DNA. These products were assembled into pBLT-2 digested with XbaI and EcoRV.
pLJ012	Overexpressing <i>dnaJ</i> , <i>dnaK</i> , <i>grpE</i> , <i>clpB</i> , <i>groES</i> , and <i>groEL</i>	A DNA fragment containing the <i>dnaJ</i> , <i>dnaK</i> , and <i>grpE</i> genes was amplified using pLJ009 as a template with primers oLJ067 (Fwd) and oLJ073 (Rev) and a fragment contain the <i>clpB</i> , <i>groES</i> , and <i>groEL</i> genes was amplified with primers oLJ074 (Fwd) and oLJ006 (Rev) using pLJ005 as a template. These products were assembled into pBLT-2 digested with XbaI and EcoRV.
pLJ013	To integrate the tac promoter upstream of <i>clpB-groES-groEL</i> and used as a template in construction of pCJ014	A DNA fragment containing the <i>clpB</i> , <i>groES</i> , and <i>groEL</i> genes was amplified using pLJ005 as a template with primers oLJ059 (Fwd) and oLJ060 (Rev), and assembled These products were assembled into pMFL160 digested with XbaI and SpeI. ¹⁷
pLJ014	Genome integration of overexpressing cassette of <i>clpB</i> , <i>groES</i> and <i>groEL</i>	The T _{SoxR} -Ptac::clpB-groES-groEL-T _{tonB} gene cassette was amplified with primers oLJ144 (Fwd) and oLJ145 (Rev) using pLJ013 as a temple. The 5' homology region was amplified from <i>P. putida</i> KT2440 genomic DNA with primers oLJ146 (Fwd), and oLJ147 (Rev), and 3' homology region was amplified with oLJ148 (Fwd) and oLJ149 (Rev). These products were assembled into pK18sB digested with SmaI and SalI.

References

1. Y. Liao, G. K. Smyth and W. Shi, *Bioinformatics*, 2013, **30**, 923-930.
2. M. I. Love, W. Huber and S. Anders, *Genome Biol.*, 2014, **15**, 550.
3. S. M. Clarkson, R. J. Giannone, D. M. Kridelbaugh, J. G. Elkins, A. M. Guss and J. K. Michener, *Appl. Environ. Microbiol.*, 2017, **83**, e01313-01317.
4. D. L. Tabb, C. G. Fernando and M. C. Chambers, *J. Proteome Res.*, 2007, **6**, 654-661.
5. Z.-Q. Ma, S. Dasari, M. C. Chambers, M. D. Litton, S. M. Sobecki, L. J. Zimmerman, P. J. Halvey, B. Schilling, P. M. Drake and B. W. Gibson, *J. Proteome Res.*, 2009, **8**, 3872-3881.
6. R. C. Edgar, *Bioinformatics*, 2010, **26**, 2460-2461.
7. V. Girish and A. Vijayalakshmi, *Indian J. Cancer*, 2004, **41**, 47.
8. I. Poblete-Castro, J. M. Borrero-de Acuña, P. I. Nikel, M. Kohlstedt and C. Wittmann, *Ind. Biotechnol.*, 2017, 299-326.
9. A. Roca, J. J. Rodríguez-Herva and J. L. Ramos, *J. Bacteriol.*, 2009, **191**, 3367-3374.
10. P. Fonseca, R. Moreno and F. Rojo, *Environmental microbiology reports*, 2011, **3**, 329-339.
11. Mary Ann Franden, Lahiru Jayakody, Wing-Jin Li, Neil J. Wagner, Bernhard Hauer, Lars M. Blank, Nick Wierckx, Janosch Klebensberger, and Gregg T. Beckham, *Metab. Eng.*, 2018, **(in revision)**
12. M. T. Guarnieri, M. A. Franden, C. W. Johnson and G. T. Beckham, *Metab. Eng. Commun.*, 2017, **4**, 22-28.
13. J. Jiménez, J. Nogales, J. García and E. Díaz, in *Handbook of hydrocarbon and lipid microbiology*, Springer, 2010, pp. 1297-1325.
14. E. Martínez-García, P. I. Nikel, T. Aparicio and V. de Lorenzo, *Microb. Cell Fact.*, 2014, **13**, 159.
15. B. A. Black, W. E. Michener, K. J. Ramirez, M. J. Bidy, B. C. Knott, M. W. Jarvis, J. Olstad, O. D. Mante, D. C. Dayton and G. T. Beckham, *ACS Sustain. Chem. Eng.*, 2016, **4**, 6815-6827.
16. A. K. Starace, B. A. Black, D. D. Lee, E. C. Palmiotti, K. A. Orton, W. E. Michener, J. ten Dam, M. J. Watson, G. T. Beckham and K. A. Magrini, *ACS Sustain. Chem. Eng.*, 2017, **5**, 11761-11769.